# APPLICATIONS OF STRESS FIELDS TO ASSESS THE BEHAVIOR AND STRENGTH OF COUPLING BEAMS SUBJECTED TO SEISMIC ACTIONS

**Sergio F. Breña**, University of Massachusetts Amherst, Amherst, MA, USA
**Miguel Fernández Ruiz**, Ecole Polytechnique Fédérale de Lausanne, Switzerland
**Aurelio Muttoni**, Ecole Polytechnique Fédérale de Lausanne, Switzerland

**ABSTRACT**

*Horizontal loading due to earthquake or wind is usually the governing action for design of reinforced concrete cores in medium to tall buildings. Building cores designed to resist these actions must be dimensioned to resist tributary vertical loads and large shear forces of varying direction and sign. Because wall cores are commonly placed around elevator shafts, openings must be left in walls to allow passage to the elevator areas. The large shears induced in the core by lateral forces have to be transmitted by beams connecting adjacent portions of the core (coupling beams). These beams usually govern both the strength and deformation capacity of the core and their structural response depends primarily on the geometry and reinforcing details chosen.*

*In this paper, the behavior and strength of coupling beams is discussed through analysis of four large-scale specimens tested at the University of Massachusetts Amherst. The specimens (2.03 × 1.65 m), representing two walls joined by a coupling beam, exhibited different failure modes depending on their slenderness and shear-to-flexural reinforcement ratio within the coupling beam region.*

*The behavior of the specimens is modeled using the stress field method to obtain realistic shear force-drift envelopes. Stress fields, in combination with strut-and-tie models, have been applied for design and detailing of members of unusual geometries subjected to monotonic loading. In this paper, a series of guidelines for applying the stress field method to members subjected to reverse cyclic loading are presented and discussed. Comparisons to test results show this technique to be a promising approach for consistent modeling of coupling beams.*

**Keywords**: Modeling: Methods and Behavior, Seismic Topics, Coupling Beams, Stress Fields, Cyclic Loading.

## INTRODUCTION

Most medium to tall buildings resist horizontal loading (earthquake or wind) through interior reinforced concrete cores (Figs. 1a,b). These horizontal actions usually govern structural design of the cores, which in turn control the deformability of the building (Fig. 1c).

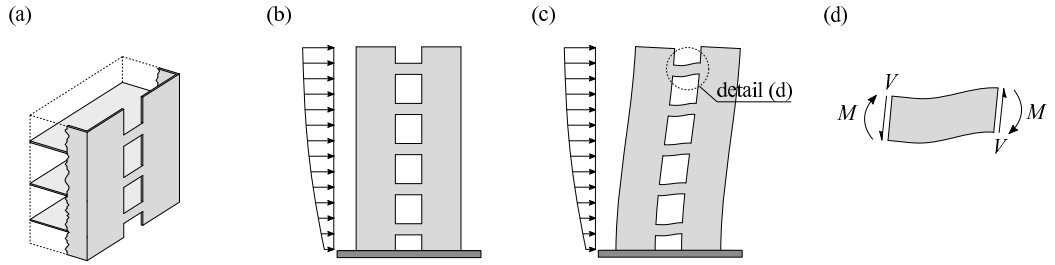


Fig. 1. Coupling beams in reinforced concrete cores: (a) view of a core with openings; (b) core subjected to horizontal loading; (c) deformation of the core; and (d) internal forces developing in a coupling beam

In order to provide access to elevators or other facilities, cores usually have aligned openings (Fig. 1a), implying that shear forces have to be carried by only limited portions of the cores (coupling beams between openings). Coupling beams are subjected to relatively large internal forces (bending and shear (Fig. 1d), causing them to be the controlling element in the overall response of the wall system (shear failure of coupling beams cause a loss in wall coupling effect).

## INFLUENCE OF GEOMETRY AND REINFORCEMENT LAYOUT ON EXPERIMENTAL BEHAVIOR OF COUPLING BEAMS

Four coupling beam specimens were tested at the University of Massachusetts Amherst with the primary intent to investigate effects of reinforcing characteristics on the observed failure mode. Specimens were designed using a concrete mix with a nominal compressive strength of 30 MPa. Nominal yield strength of the longitudinal and transverse reinforcement was 410 MPa, except for specimen CB-2 that had transverse reinforcement consisting of deformed wire with a nominal yield strength of 580 MPa. Table 2 lists the main geometric and as-built material properties of all specimens. Figure 2 illustrates the geometry and reinforcement patterns of the four specimens tested in this research. Only coupling beams with orthogonally placed reinforcement were studied. As observed, the main parameters investigated were beam span, transverse reinforcement content, and longitudinal reinforcement content. Full details of the specimens were presented by Ihtiyar and Breña[1].

Shear forces were generated in the coupling beams by applying horizontal forces to two stiff concrete walls constructed on each end of the specimens. Horizontal loading was distributed to the top of the walls using a stiff steel element that imposed equal lateral displacement to both walls (Fig. 3). Given the geometry of the test setup, an applied lateral force $Q$ generated shear forces at the ends of the coupling beams equal to $Q.h_{pin}/(l_b+l_w)$, giving shears of 1.1 and 0.8 times $Q$ for the short (CB-1 and CB-3) and long (CB-2 and CB-4) specimens,

respectively. Lateral force was applied cyclically in sets of three cycles at pre-defined amplitudes. Applied loading was force-controlled in pre-yield stages and subsequently changed to displacement control at post-yield stages. At loading stages below the estimated yield shear force ($V_y$), the applied loading amplitudes were 1/3, 2/3, and 3/3 of $V_y$. The lateral displacement at the top of the walls at $V_y$ was defined as the displacement at yield. Subsequent loading was applied in increments of 0.5 times the yield displacement. Loading was stopped as specimens began to lose strength at higher applied displacements since the primary intent was to determine the stiffness of the loading branch and the factors contributing to coupling beam deformation. Only specimen CB-4 was taken to much higher displacements because it was designed to be flexurally dominated and its shear retention capacity at large displacements (residual strength) was of particular interest.

Table 2. Primary as-built parameters of coupling beam specimens

| Specimen | $d$ | $l_n$ | Longitudinal steel | | | Transverse steel | | | $f_c$ |
|---|---|---|---|---|---|---|---|---|---|
| | | | $A_s$ | $f_{yl}$ | $\rho_l$[(a)] | $A_v$ | $f_{yt}$ | $\rho_v$ | |
| | [mm] | [mm] | [mm$^2$] | [MPa] | [%] | [mm$^2$] | [MPa] | [%] | [MPa] |
| CB-1 | 340 | 510 | 600 | 517 | 0.69 | 142 | 524 | 1.1 | 39 |
| CB-2 | 340 | 1020 | 851 | 448 | 0.99 | 52 | 607 | 0.13 | 39 |
| CB-3 | 270 | 510 | 860[(b)] | 517 | 1.25 | 142 | 524 | 1.1 | 31 |
| CB-4 | 340 | 1020 | 400 | 517 | 0.47 | 142 | 524 | 1.1 | 30 |

[(a)] $\rho_l = A_s/bd$; $\rho_v = A_v/b_w s$; [(b)] Includes lowermost layer of distributed longitudinal web reinforcement (2 No. 4 bars, Fig. 2a).

## SHEAR FORCE-CHORD ROTATION RESPONSE

Specimen response was primarily evaluated by examining the shear force-chord rotation response. Only specimen CB-2 was designed to have insufficient shear strength ($V_n$) to develop yielding of the longitudinal reinforcement according to ACI 318 shear strength equations for wall segments (ACI 318-08[2], Eq. 21-7). All other specimens were expected to be able to develop flexural yielding and attainement of flexural strength ($V_f$) at the ends of the beams. Plastic hinging was not expected for any specimen except CB-4 (with low flexural reinforcement ratio and a relatively long span). The primary force-deformation parameters measured during the tests are listed in Table 3.

Table 3. Summary of measured shear force and chord rotation in beams

| Specimen | $Q_{test,pk}$ [kN] | $V_{y,test}$[(a)] [kN] | $\theta_{y,test}$ [rad] | $V_{test,pk}$ [kN] | $\theta_{test,pk}$ [rad] | $V_f$ [kN] | $V_n$[(b)] [kN] |
|---|---|---|---|---|---|---|---|
| CB-1 | 436 | 371 | 0.0154 | 480 | 0.0311 | 492 | 709 |
| CB-2 | 344 | 227 | 0.0057 | 275 | 0.0076 | 319 | 187 |
| CB-3 | 460 | 447 | 0.0211 | 506 | 0.0299 | 575 | 693 |
| CB-4 | 300 | 141 | 0.0050 | 240 | 0.0214 | 168 | 647 |

[(a)] Determined using strain gauges on flexural bars; [(b)] Based on ACI 318-08[2] Eq. (21-7)

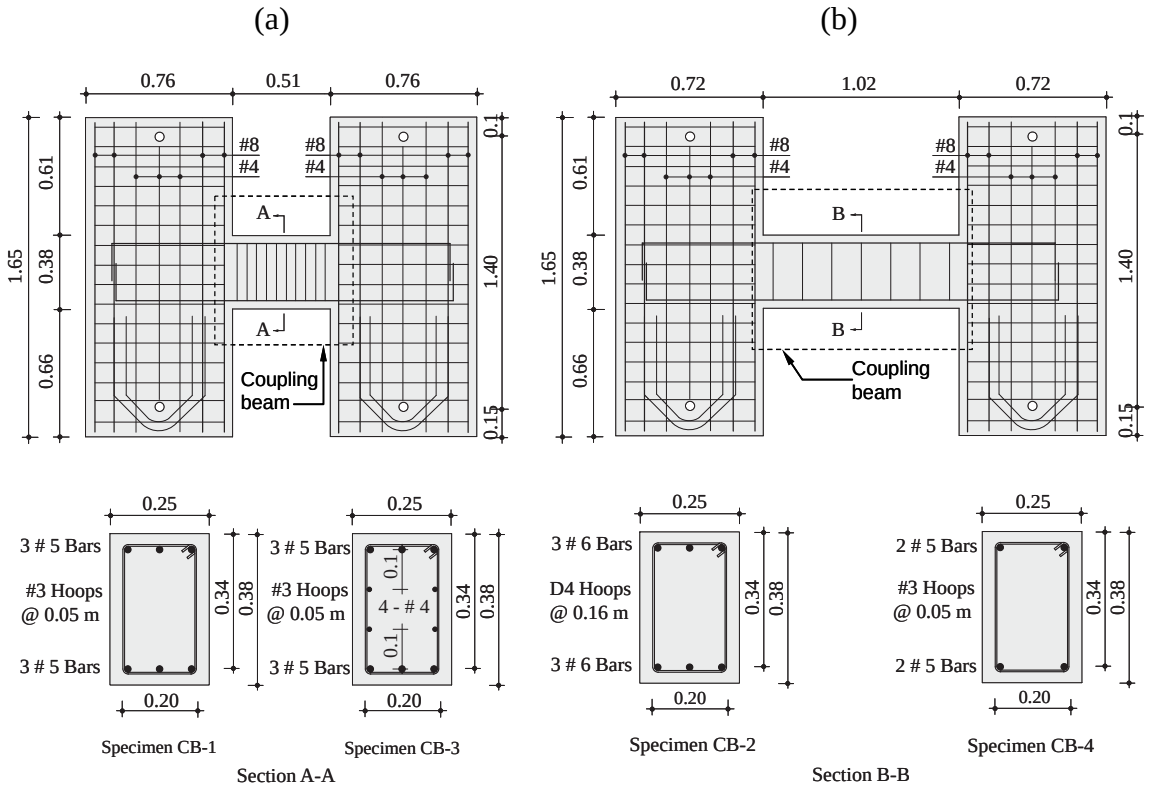


Fig. 2. Specimen geometry and reinforcing details (dimensions in [m]): (a) specimens CB-1 and CB-3; and (b) specimens CB-2 and CB-4

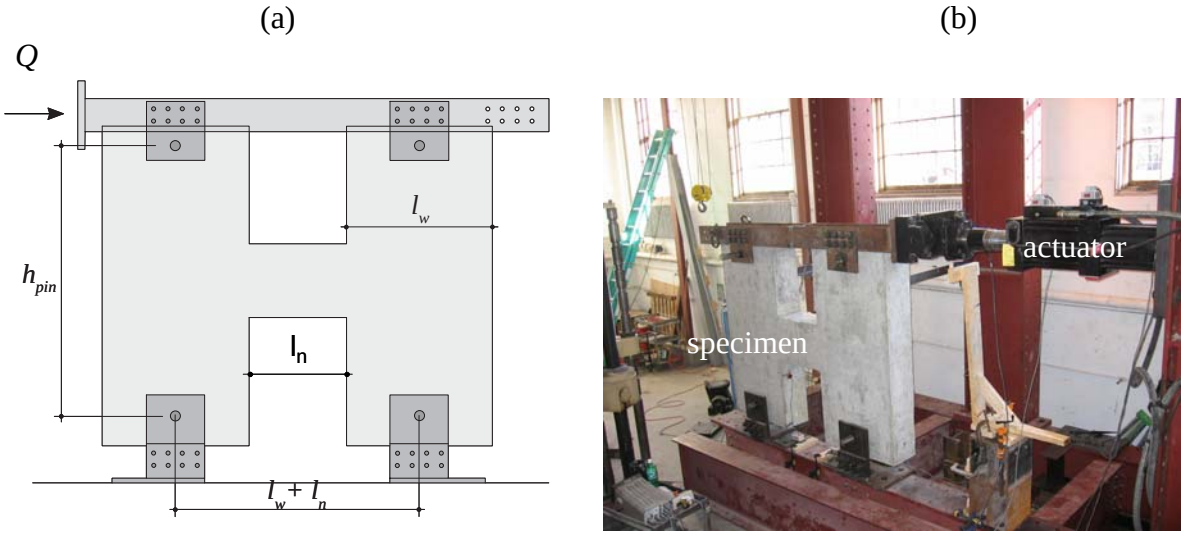


Fig. 3. Experimental setup: (a) geometry and (b) specimen in testing rig

The cyclic shear force-chord rotation behavior of the four beams tested in the experimental program are shown in Fig. 4, from which several response features can be highlighted. Specimens CB-1 and CB-3 (short span) exhibited essentially similar cyclic characteristics.

Both specimens reached approximately the same shear force and were able to develop similar chord rotations at yield and peak shear force. The influence of horizontal web reinforcement in CB-3 did not affect the general characteristics of the hysteretic response significantly, but did increase the measured chord rotation at yield.

The highly contrasting behavior of specimens CB-2 and CB-4, although with the same span-to-depth ratio, was primarily caused by the significantly different amounts of transverse reinforcement. Transverse reinforcement in CB-2 was barely sufficient to maintain shear strength after formation of the first diagonal crack and resulted in a brittle failure mode with no yielding of the longitudinal reinforcement. On the other hand, CB-4 had a very ductile response as a result of low flexural strength ($V_f$) and relatively high shear capacity ($V_n$). Specimen CB-4 was the only beam that had a higher shear strength than required to develop plastic hinging and spread of plasticity near beam ends.

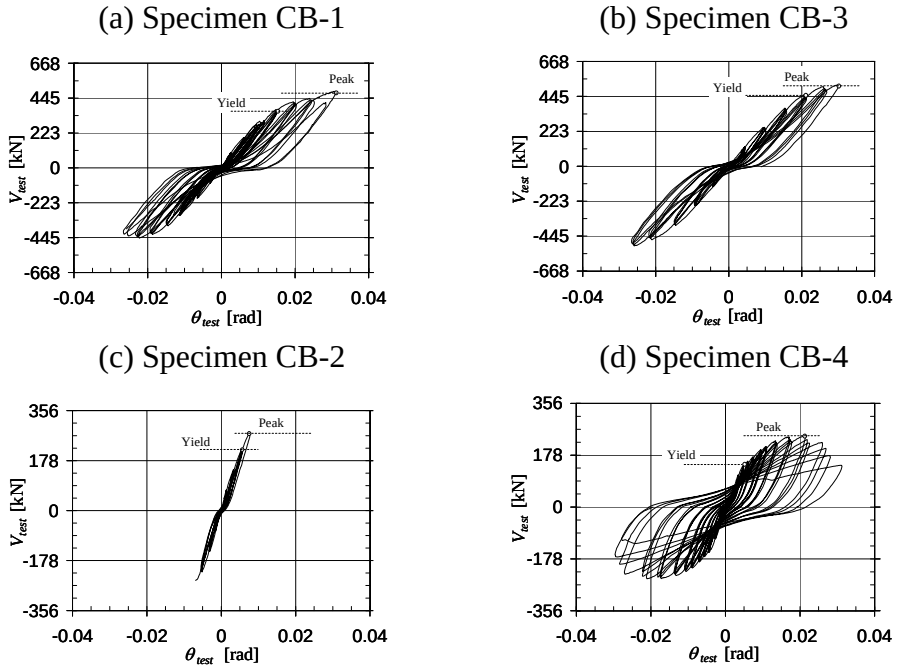


Fig. 4. Cyclic shear force-chord rotation response of coupling beam specimens

## STRESS FIELD MODELS TO ESTIMATE THE PEAK FORCE AND INITIAL STIFFNESS OF COUPLING BEAM SPECIMENS

Performance evaluation of existing buildings relies on techniques to estimate the response characteristics of the components of the structural system. Stiffness and strength estimates of coupling beams obtained using available procedures have been found to sometimes correlate poorly with actual response depending on reinforcement configuration and failure mode. Stress field modeling is investigated as a tool to improve estimation of these values as needed in the context of performance-based engineering[3].

## STRESS FIELDS FOR MODELING OF REINFORCED CONCRETE SHEAR WALLS

Stress fields were developed from direct application of the lower bound theorem of the theory of plasticity to reinforced concrete members by Drucker[4]. Original stress field models used the assumption of rigid-plastic material behavior (Figs. 5a,b). These stress fields, termed rigid-plastic (discontinuous) stress fields, provide safe estimates of the failure load and allow the designer to have a clear understanding of the load-carrying mechanisms of a structure. Application of rigid-plastic stress fields has two drawbacks[5]. First, there is no unique solution to a given problem so a certain level of experience is needed to choose the most adequate load-carrying mechanism for a particular structure. Second, given the assumption of rigid-plastic material behavior, deformation capacity of the structural member cannot be estimated. This last drawback limits the used of rigid-plastic stress fields for solution of problems that require accurate estimates of deformation parameters such as for elements subjected to seismic loading.

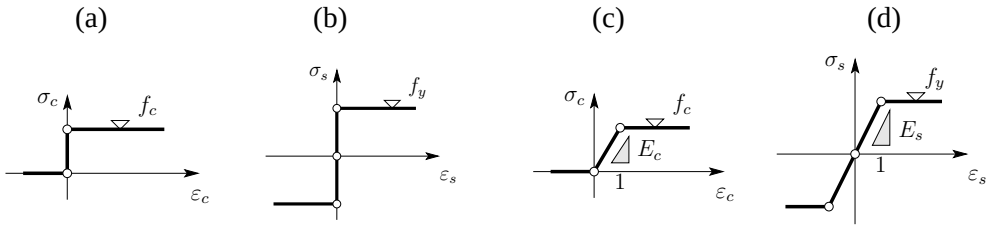


Fig. 5. Constitutive laws for stress field modeling: (a) rigid-plastic constitutive law for concrete; (b) rigid-plastic constitutive law for steel; (c) elastic-plastic constitutive law for concrete; and (d) elastic-plastic constitutive law for steel

In order to overcome these two limitations, elastic-plastic (continuous) stress fields have recently been developed by Fernández Ruiz and Muttoni[5]. These models were developed assuming that materials have an elastic-plastic constitutive relation (Figs. 5c,d). With this assumption the strains in concrete and steel can be calculated and the displacements of the structural element can be determined. Since the principal strains in concrete are known, the influence of transverse strains on the compressive strength of concrete can be considered using relationships that account for reduction of compressive strength as a function of increasing transverse strain such as the one proposed by Vecchio and Collins[6]. An efficient implementation of continuous stress fields using the finite element method is described and discussed by Fernández Ruiz and Muttoni[5].

## COMPARISON OF ELASTIC-PLASTIC STRESS FIELDS WITH COUPLING BEAM TESTS

Results from the application of elastic-plastic stress fields to the coupling beam tests discussed previously are presented in this section. Figure 6 shows the calculated stress fields at peak load for the four coupling beam specimens tested in the laboratory. The stress fields are consistent with the cracking patterns observed during the tests and are therefore considered representative of the actual force path. Figure 7 shows shear force – chord rotation envelopes for the four specimens calculated using the measured material properties (Table 2). Also, in the same figure, the calculated shear force – chord rotation envelope is

plotted assuming a reduced modulus of concrete, equal to one-quarter of the one determined using measured concrete strength, to simulate the reduction in shear stiffness of coupling beams after cracking. A summary of results for both analyses are listed in Table 5.

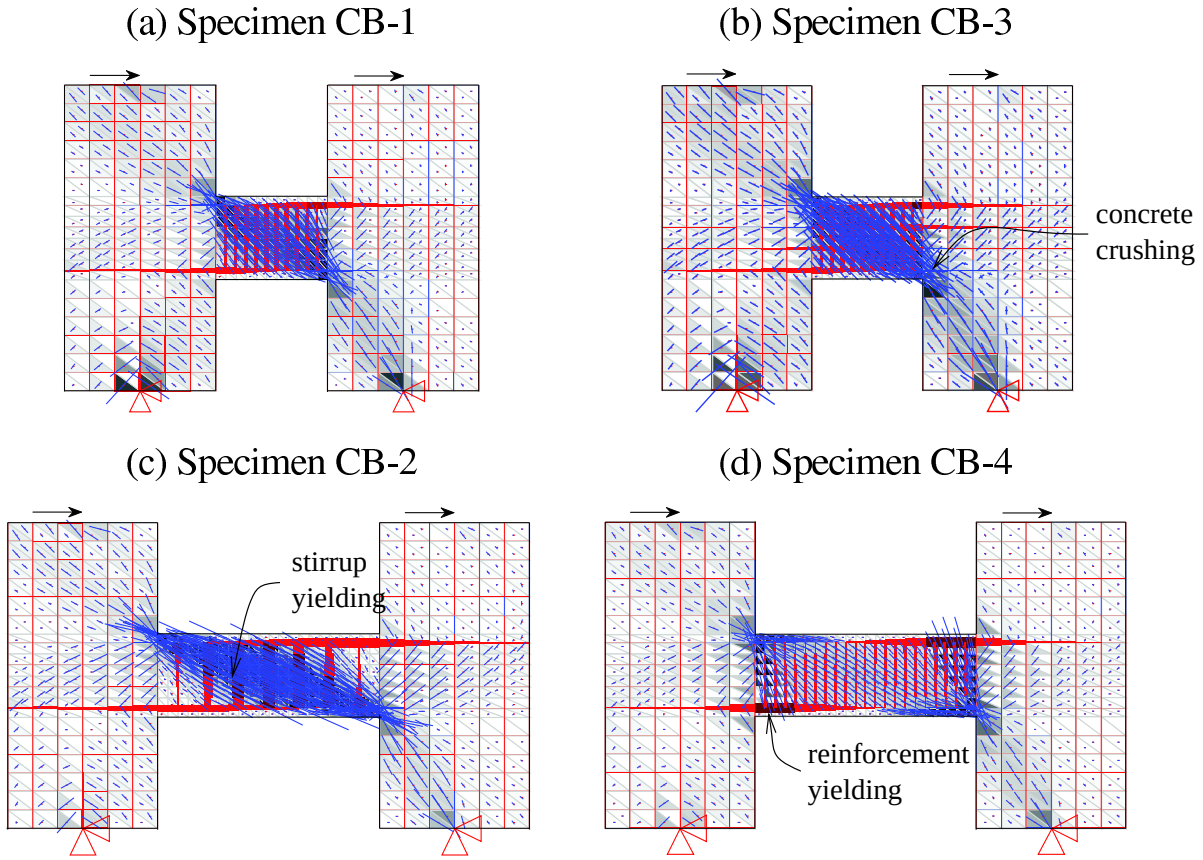


Fig. 6. Elastic-plastic stress fields obtained for coupling beam specimens

A comparison between the test results and shear force – chord rotation envelopes calculated using continuous stress field modeling leads to the following observations:

1. Failure loads are accurately predicted for all members, regardless of the slenderness, reinforcement layout and failure mode.

2. Failure loads are hardly sensitive to reductions in the modulus of elasticity of concrete. Nevertheless, small reductions in the failure load were obtained for softer modulus of elasticity. This is caused by development of higher transverse strains leading to larger concrete strength reductions[6].

3. Chord rotations are accurately estimated using the elastic (uncracked) modulus of elasticity of concrete during the initial cycles of loading. Degradation in the modulus of elasticity due to cyclic loading plays a significant role in the deformational behavior for large displacements. This is confirmed by a better match between calculated force-deformation envelopes and measured cyclic response in particular for shorter elements when reducing the modulus to $E_c/4$.

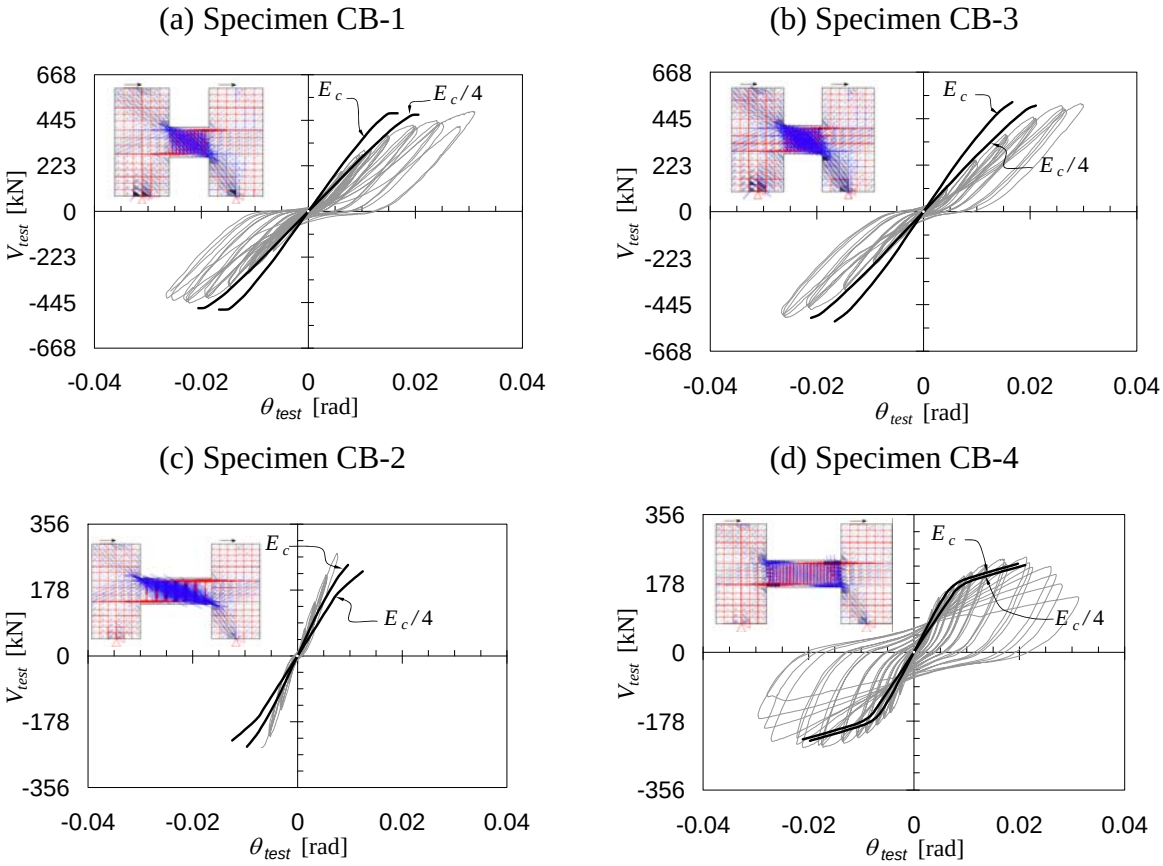


Fig. 7. Comparison of shear force – chord rotation envelopes using elastic-plastic stress fields with measured response

Table 5. Comparison of measured and calculated failure loads and chord rotations at maximum load (values in parentheses obtained using an effective modulus of elasticity of concrete equal to $E_c/4$).

| Specimen | $V_{test\text{-}pk}$ [kN] | $\theta_{test\text{-}pk}$ [rad] | $V_{calc}$ [kN] | $\theta_{calc}$ [rad] | $\frac{V_{test}}{V_{calc}}$ | $\frac{\theta_{test}}{\theta_{calc}}$ |
|---|---|---|---|---|---|---|
| CB-1 | 480 | 0.0311 | 479 | 0.0167 | 1.00 | 1.86 |
| | | | (472) | (0.0206) | (1.02) | (1.51) |
| CB-2 | 275 | 0.0076 | 246 | 0.0096 | 1.12 | 0.79 |
| | | | (229) | (0.0125) | (1.20) | (0.61) |
| CB-3 | 506 | 0.0299 | 524 | 0.0166 | 0.97 | 1.80 |
| | | | (508) | (0.0211) | (1.00) | (1.42) |
| CB-4 | 240 | 0.0214 | 228 | 0.0197 | 1.05 | 1.09 |
| | | | (225) | (0.0211) | (1.07) | (1.01) |
| | | | | Average | 1.03 | 1.39 |
| | | | | | (1.07) | (1.14) |
| | | | | CoV | 0.06 | 0.38 |
| | | | | | (0.09) | (0.36) |

The results show that stress field modeling is a promising technique that can capture the backbone behavior of coupling beams. It allows use of a consistent approach that accounts for the various mechanical and geometric properties of a structure without needing to specify a large number of parameters or relying on a large numbe of hypotheses. The reduction in stiffness used in this paper (one quarter of the elastic one) for coupling beams subjected to large displacements is rather crude. It was used to better approximate observed behavior and will be refined in subsequent research. This stiffness reduction, however, is consistent with values that other researchers have observed for relatively short deep coupling beams (Paulay[7]; Park and Ang[8]; Ihtiyar and Breña[9]).

## FUTURE WORK

The authors are currently working on a formulation to compute coupling beam stiffness degradation as a function of concrete loading history (number of cycles and maximum deformation demand). This work will allow automatic development of elastic-plastic stress fields for development of backbone envelope curves for use in performance-based seismic design or assessment, and improvement of chord rotation estimates.

## CONCLUSIONS

This paper compares the load and stiffness of four large-scale coupling beams tested in the laboratory with results obtained using elastic-plastic stress field models. The beams were subjected to cyclic loading, had different reinforcing bar layouts, and two different aspect ratios. The tests were designed to capture differences in behavior associated to geometry and reinforcing layout. The main conclusions from this research are:

1. Slenderness, reinforcement layout, amount of transverse reinforcement and failure mode (bending or shear) have a significant influence on the strength and behavior (deformation capacity) of coupling beams.

2. Modeling the envelope response of coupling beams based on elastic-plastic stress fields provides a rational approach for estimating strength and deformation capacity at yield and peak load. This technique allows accounting for the influence of the various mechanical and geometric parameters on behavior.

3. Stiffness degradation of concrete subjected to cyclic loading with large amplitudes plays a significant role in the shear force – chord rotation relationship of coupling beams. This degradation should be considered in future development of more accurate predictive models used for estimation of envelope response.

## ACKNOWLEDGEMENTS

The authors would like to acknowledge Onur Ihtiyar for performing the experimental work described in this paper as part of his Masters thesis at the University of Massachusetts Amherst during 2007 and Dr. Neven Kostic for his assistance with stress field modeling of

the coupling beam specimens described in this paper.

## REFERENCES

1. Ihtiyar, O. and Breña, S.F. (2007). "Assessment of FEMA 356 Techniques for Orthogonally Reinforced Coupling Beams through Experimental Testing." *2007 ASCE Structures Congress: Structural Engineering Research Frontiers*. Long Beach, CA.
2. American Concrete Institute (ACI) (2008). "Building Code Requirements for Structural Concrete (318-08) and Commentary (318R-08).", *ACI 318-08*, Detroit, MI.
3. Breña, S.F., Fernández Ruiz, M., Kostic, N. and Muttoni A. (2009). "Modelling techniques to describe the backbone curves of r/c coupling beams subjected to seismic loading" *Studies and Researches*, Vol. 29, 2009, accepted for publication
4. Drucker, D. C. (1961). "On Structural Concrete and the Theorems of Limit Analysis." *Publications, International Association for Bridge and Structural Engineering*. Vol. 21, pp. 49-59.
5. Fernández-Ruiz, M., and Muttoni, A. (2007). "On Development of Suitable Stress Fields for Structural Concrete." *ACI Structural Journal*. Vol. 104, No. 4, pp. 495-502.
6. Vecchio, F. J. and Collins, M. P. (1986) "The modified compression field theory for reinforced concrete elements subjected to shear", *ACI Journal*, Vol. 83, No. 2, March-April, 1986, pp. 219-231.
7. Paulay, T. (1971a). "Coupling Beams of Reinforced Concrete Shear Walls." *Journal of the Structural Division, Proceedings ASCE*. Vol. 97, No. ST3, pp. 843-861.
8. Park, Y-J, and Ang, A.H-S. (1985). "Mechanistic seismic damage model for reinforced concrete." *Journal of Structural Engineering*, Vol. 111, No. 4, pp. 722-739.
9. Ihtiyar, O. and Breña, S.F. (2006). "Force-Deformation Response of Conventionally Reinforced Coupling Beams: Evaluation of FEMA 356 and FEMA 306." *2006 8th U.S. National Conference on Earthquake Engineering*. Paper no. 701. San Francisco, CA.